Climate Dynamics (2020) 54:4005–4020
https://doi.org/10.1007/s00382-020-05215-4

Swapping of the Pacific and Atlantic Niño influences on north central India summer monsoon

Ramesh Kumar Yadav[1,2,3] · S.-Y. Simon Wang[1,2] · Chi-Hua Wu[4] · Robert R. Gillies[1,2]

Received: 16 July 2019 / Accepted: 13 March 2020 / Published online: 24 March 2020

Abstract
The highly populated north central India receives 90% of annual rainfall during June to September. The interannual variation of summer monsoon rainfall is less studied compared to central and western India, due to its weak signal with the El-Niño-Southern Oscillation (ENSO). Previous studies have reported a marked decadal variation in the ENSO influences on north India rainfall, but the teleconnections of this variation are not satisfactorily understood. A pathway of the changing ENSO influences on north central India rainfall is revealed from observational data analysis and numerical experiments. While La Niña-like conditions produce anomalous northeasterly wind over India and reduce the tropospheric wind shear, the emergence of the Atlantic Niño appears to overtake this ENSO influence. The Atlantic Niño intensifies the meridional stationary wave affecting pressure anomaly over northwest Europe. This excites the Eurasian Rossby wave train along the mid-latitude producing upper-troposphere high pressure anomaly, subsequently affecting north India. Future work should examine the extent to which these teleconnections are represented in climate forecast models to aid the seasonal prediction of north central India rainfall.

Keywords Indian summer monsoon · North India · ENSO · Atlantic Niño Deep convection Sea surface temperature · Pressure anomaly

1 Introduction

The north central part of India includes fertile regions of the Gangetic Plain where population density is substantial. Agriculture and animal husbandry comprises the main occupations in the north central India; these rely heavily on a sustained rainfall during the Indian Summer Monsoon (ISM) from June to September (JJAS). Recent study by Yadav and Roxy (2019) has shown that the post-2002 increase in the Indian summer monsoon rain observed by Jin and Wang (2017), has not taken place in this region. Analysis of the seasonal JJAS India rainfall for the period 1979–2017 had shown a big patch of the drying trend over the plains of north central India that consists of Bihar and East Uttar Pradesh. The study also reveals that this region is largely independent of the monsoon rainfall variability in central India or northeast India. Therefore, these two meteorological subdivisions in northern India, Bihar and East Uttar Pradesh (Fig. 1), are considered for this study. The ISM in these two provinces exhibits inconsistent variations with its southern counterpart (e.g., Ding and Wang 2005). Despite the wealth of literature that pertains to the study of the ISM, the ISM impacts for north central India (especially in Bihar and East Uttar Pradesh) have been overlooked which, given its importance to the livelihood of the population residing there, is an omission that we address here.

The northward movement of the monsoon trough from its climatological position and its interaction between the westerly trough and the monsoonal flow collectively affect northern India's summer rainfall, herein "northern ISM" (Ramaswamy 1956, 1962; Ramamurthy 1969; Krishnamurti et al. 1980; Raman and Rao 1981; Vellore et al. 2014). It has been documented that the prominent impact

✉ Ramesh Kumar Yadav
yadav@tropmet.res.in

1 Plants, Soils and Climate Department, Utah State University, Logan, Utah, USA

2 Utah Climate Center, Utah State University, Logan, Utah, USA

3 Indian Institute of Tropical Meteorology, Pashan, Pune 411008, India

4 Research Center for Environmental Changes, Academia Sinica, Taibei, Taiwan

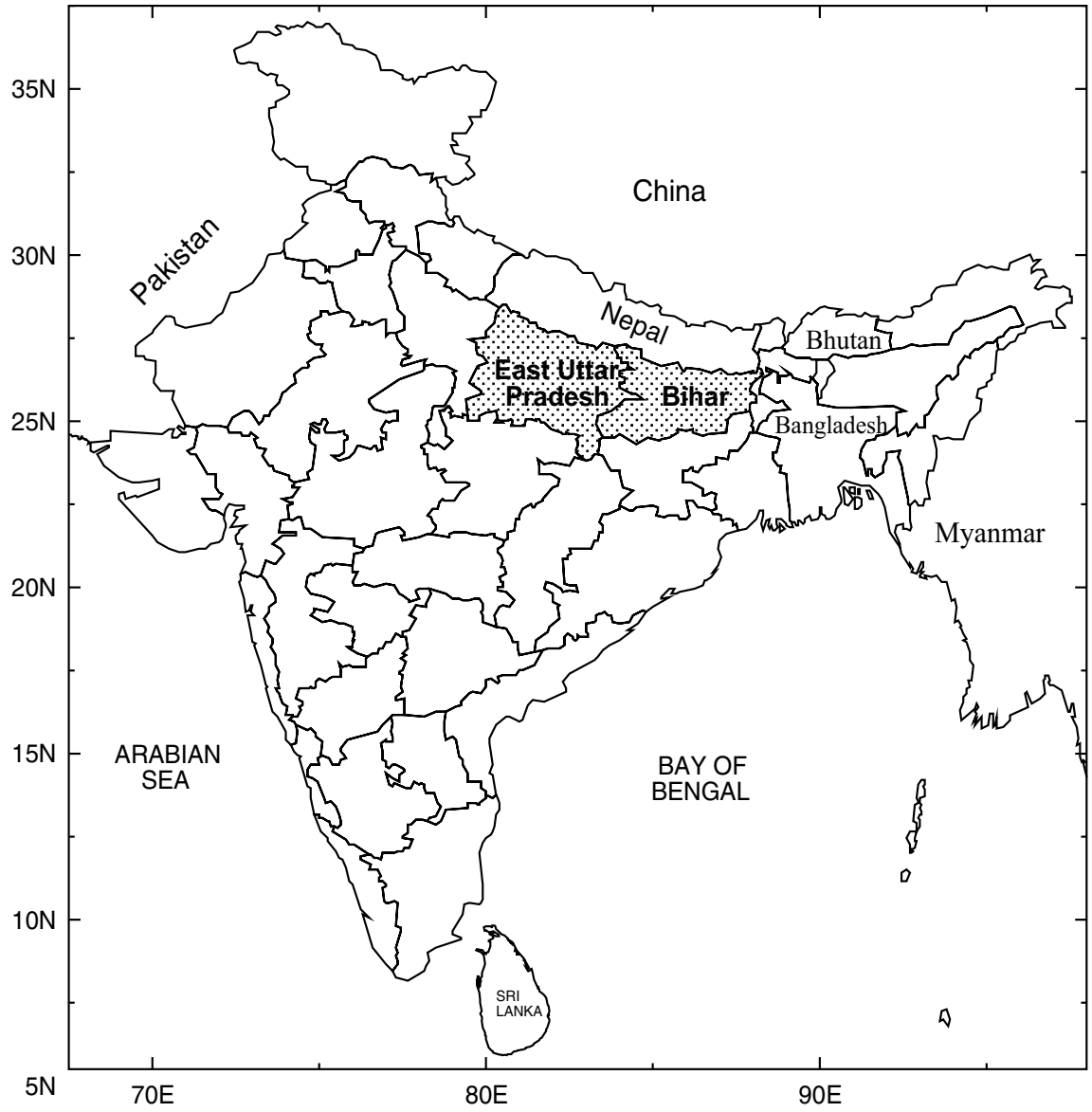

Fig. 1 Shaded regions are two meteorological sub-divisions of India: East Uttar Pradesh and Bihar, considered for the study of north central India summer monsoon rainfall

of El-Niño-Southern Oscillation (ENSO) on the broad ISM underwent a change around the late-1970s in response to a major climate shift observed in the Indo-Pacific Ocean (Graham 1994; Trenberth and Hurrell 1994; Yadav 2009a). The ENSO–ISM relationship has transformed from one that was primarily driven by the east Pacific El Niño to one by the central Pacific El Niño (Krishna Kumar et al. 2006). Additionally, recent research has highlighted the importance of the Atlantic Niño and its interaction with the north central India ISM (Kucharski et al. 2008; Yadav 2017b; Yadav et al. 2018); this interaction induces changes in the Indian Ocean SST along the eastern coast of Africa and in the western Indian Ocean basin (Kucharski et al. 2008). Moreover, the Atlantic's impact on the north central ISM also forms through the Eurasian atmospheric wave trains (Ding and Wang 2005, 2007; Yadav 2009a, b, 2017; Yadav et al. 2018).

The southern parts of India exhibit a circulation pattern that is mostly of a tropical nature, while the northern parts of India are influenced through interaction between the tropical and extra-tropical circulations (Ding and Wang 2009; Wang et al. 2011). What is more, the ENSO influence on northern India is not stable, having pronounced decadal variations in the ENSO-ISM relationship (e.g., Torrence and Webster 1999; Krishna Kumar et al. 1999; Krishnamurthy and Goswami 2000; Kinter et al. 2002; Annamalai and Liu 2005; Gershunov et al. 2001). Due to this decadal variation, diverse

teleconnection patterns have been observed: For instance, a study done by Yadav et al. (2018) with data after late-1970s showed that the Atlantic Niño significantly influences northern Indian rainfall in a east-west dipole pattern across India; this is different from previous thoughts (e.g., Kucharski et al. 2008) that considered the ISM rainfall homogeneously but did not separate the anti-correlated northwestern and northeastern rainfall regimes. While Kucharski et al. (2008) did mention the tropical circulation perturbation and the Atlantic Niño, they did not include the mid-latitude disturbances that evidentially affect the northern Indian rainfall variability. In this study, we explored the processes responsible for the previously documented reduction of ENSO influences on northern ISM through examination of the decadal variation in the teleconnections and the distinctive circulation patterns. The data and methods are described in Sect. 2. The results are presented in Sect. 3, and finally the conclusion and discussion in the last section.

2 Data and model

Monthly Indian meteorological subdivisions of rainfall data from June to September (JJAS), for the period 1948–2016 (69-years), were obtained from the Indian Institute of Tropical Meteorology records (Parthasarathy et al. 1995; available at http://www.tropmet.res.in). Rainfall records from 37 raingauges within the Bihar and East Uttar Pradesh sub-divisions were acquired for the purposes of this study. Other data resources used included NCEP/NCAR reanalysis data (Kalnay et al. 1996) and monthly sea surface temperatures (SST) from the ERSST version 5 data set (Huang et al. 2017). The NCEP/NCAR reanalysis is the only full atmospheric assimilation dataset available to study this secular relationship from 1948 onwards, based on the in-situ observational records. For spatial plotting of rainfall, we have used gridded (0.25°) rainfall data from the India Meteorological Department (Pai et al. 2014).

All the data series, except for the trend analysis, were detrended before carrying out any correlation and regression analysis in order to highlight inter-annual and inter-decadal variations. Excess and deficient years were defined if the standardized values were greater than + 1 and less than − 1, respectively. We also used a simplified general circulation model (Simplified Parameterizations, privitivE-Equation DYnamics, SPEEDY), developed at the International Centre for Theoretical Physics (ICTP) (Molteni 2003; Kucharski et al. 2006), to investigate potential atmospheric responses to SST anomalies. Although the eight-vertical-layer SPEEDY model conducted at longitude/latitude resolution by 3.75° might inevitably include unrealistic topographic effects, it can capture the major circulation features of South Asian summer monsoon, including particularly the seasonal migration of large-scale circulation (Wu et al. 2018). The integration length of the SPEEDY model simulations was 50 years and the latest 30 years were analyzed (Table 1).

3 Results

3.1 The state of change

The area weighted average rainfall of north central ISM is shown in Fig. 2a for the period of 1948–2016, revealing

Table List of acronyms used in the paper

Acronyms	Description
BoB	Bay-of-Bengal
CGT	Circum-global teleconnection
ENSO	El-Niño-Southern Oscillation
ERSST	Extended reconstructed sea surface temperature
GPH	Geo-potential height
ISM	Indian summer monsoon
ITCZ	Inter tropical convergence zone
JJAS	June to September
MSLP	Mean sea level pressure
NCEP/NCAR	The National Centers for Environmental Prediction (NCEP) and the National Center for Atmospheric Research (NCAR)
SAD	Sub-tropical south Atlantic dipole
SPCZ	South Pacific convergence zone
SPEEDY	Simplified parameterizations, privitive-equation dynamics
SST	Sea surface temperature
TPD	Tropical Pacific Dipole between northeast of Australia and north of equatorial central Pacific

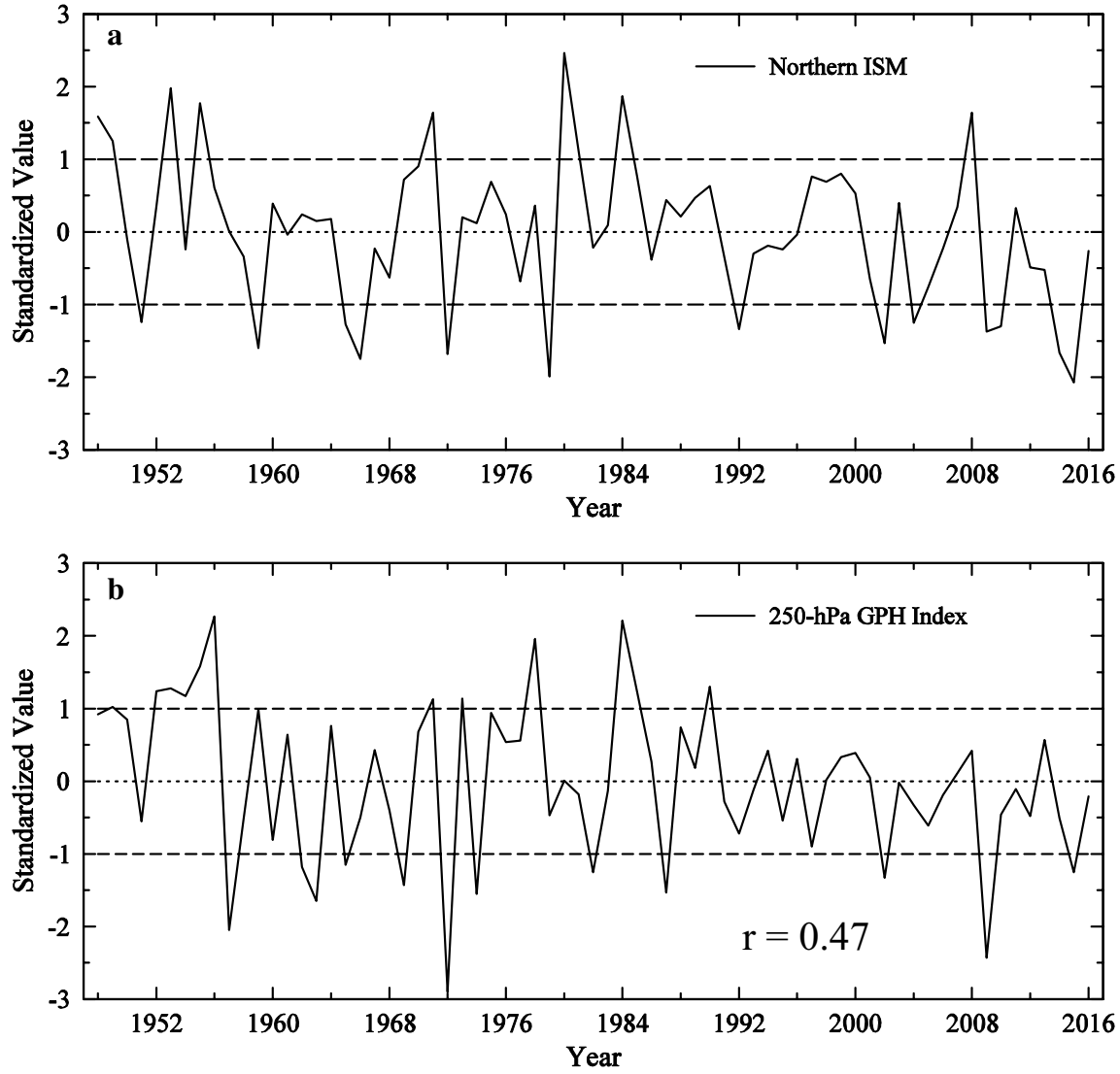

Fig. 2 Standardized time series of (**a**) north central ISM and (**b**) 250-hPa GPH index for the1948-2016 period. The standardized values greater and lower than + 1 and − 1 represents theexcess and deficient years, respectively. The horizontal dashed lines are + 1 and − 1 standardized values

marked inter-annual variability. We computed the contiguous correlation patterns of the north central ISM rainfall with (a) SST, mean sea level pressure (MSLP) and 850-hPa winds, and (b) 250-hPa geo-potential height (GPH) and winds, for the 1948–2016 period and shown in Fig. 3. The correlation of low-level circulation features shows a La Niña-type pattern in the Pacific, exhibiting a SST dipole with strong negative correlations of SST over north equatorial Pacific and a positive correlation center northeast of Australia. The north-east of Australia describes the position of 'south Pacific convergence zone' (SPCZ) and the north of equatorial Pacific box represents the 'inter tropical convergence zone' (ITCZ) at the central Pacific. The mean SPCZ tends to lie over a region of large SST gradient, while ITCZ over a maximum of SST (Fig. 6). Both SPCZ and ITCZ are inter-related to each other. La Niña-like conditions with weakening of ITCZ is associated with a southwestward displacement of the SPCZ. On the other hand, El Niño-like condition with intense ITCZ is associated with a northeastward displacement of the SPCZ (Folland et al. 2002). Also, La Niña-like condition is associated with strong trade winds that result in upwelling of cold deep water in the large areas due to divergence and vice-versa for El Niño-like condition. Therefore the SST correlation over equatorial central Pacific is much larger than north-east of Australia. The MSLP shows a strong positive correlation in the north Pacific and, the tropical central and eastern Pacific; this is associated with an anti-cyclonic circulation anomaly over the north Pacific. Significant anomalous south/southeasterly winds from Bay-of-Bengal (BoB) and northerly winds

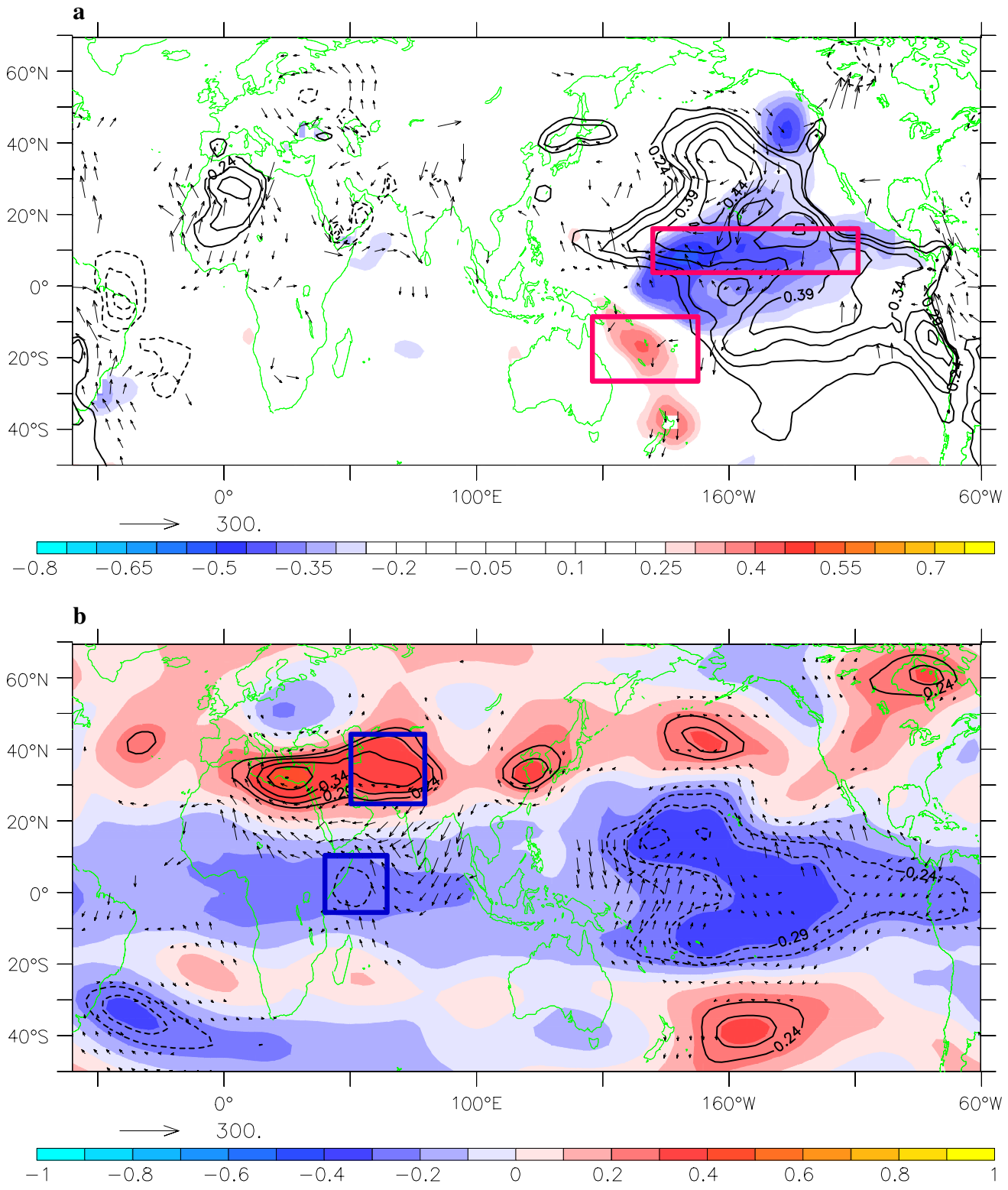

Fig. 3 **a** Contiguous correlation of north central ISM with (**a**) SST (shaded), MSLP (contours) and regression of 850 hPa wind (arrows; m/s) onto north central ISM and (**b**) 250-hPa geopotential (color shade and contours above 95% significant level) and regression of 250-hPa wind (arrows; m/s) onto north central ISM. The pink boxes in (**a**) represents the tropical Pacific dipole (TPD). The blue boxes in (**b**) are considered for calculating the pressure gradient at 250-hPa level

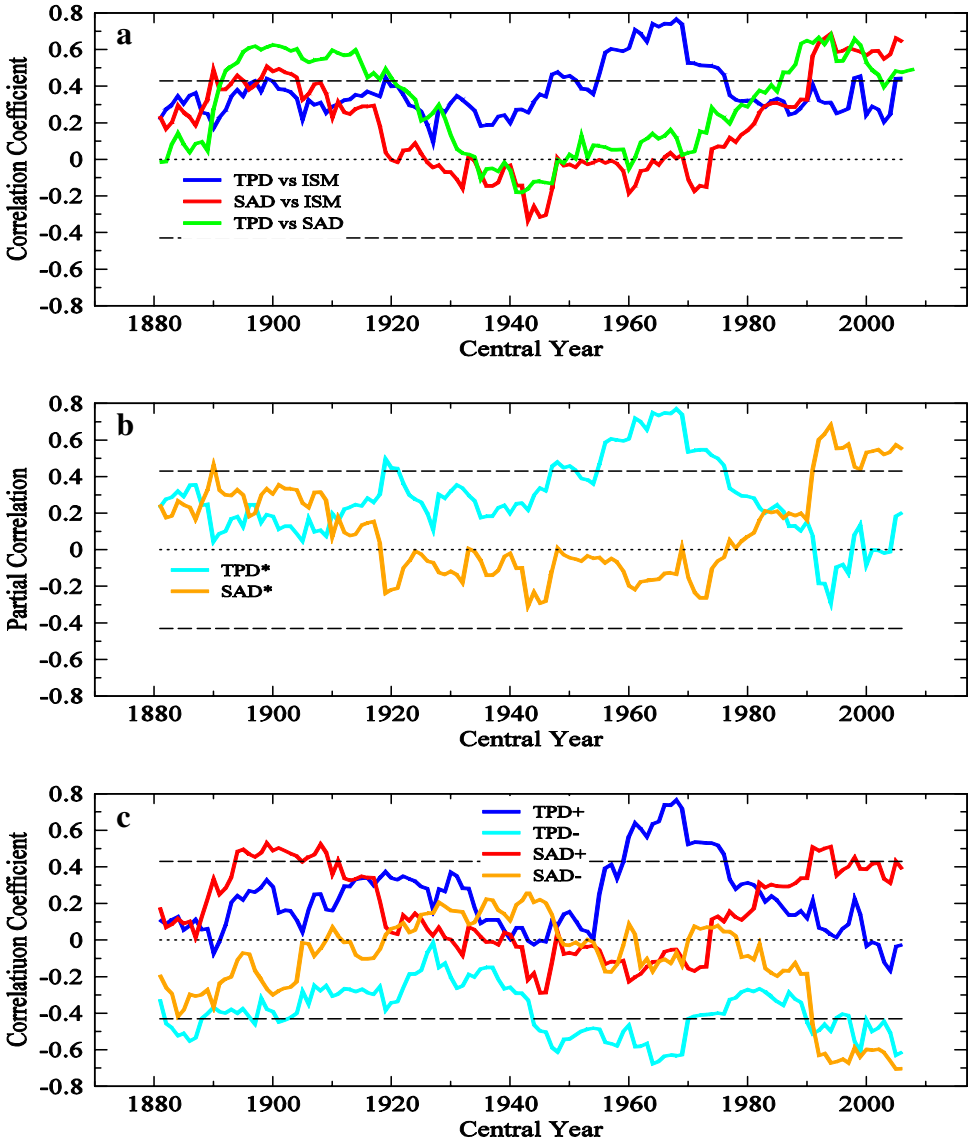

Fig. 4 **a** Correlation on 21-year moving window of north central ISM with tropical Pacific dipole (TPD; blue line) and south Atlantic dipole (SAD; red line), and between TPD and SAD (green line), **b** partial correlation on 21-year moving window of north central ISM with tropical Pacific dipole (TPD*; cyan line) and south Atlantic dipole (SAD*; orange line) after removing the contribution of SAD and TPD, respectively, and **c** 21-year sliding correlation of each of the dipole indexes with north central ISM (positive TPD; blue line), (negative TPD; cyan line), (positive SAD; red line) and (negative SAD; orange line)

from north of India are converging towards north central ISM region acting as the source of moisture supply. Correspondingly, the 250-hPa GPH (Fig. 3b) shows significant negative correlation over tropical Pacific and west tropical Indian Ocean and patches of significant positive correlation along the mid-latitude/extra-tropical regions (20°N–50°N), with strong positive correlation over northwest of India and east Mediterranean. The significant high pressure anomaly over east Asia, North Pacific and North Atlantic, represents a circum-global teleconnection (CGT) pattern with high zonal wave number; this was first noted Hoskins and Ambrizzi (1993), Ambrizzi et al. (1995) and later was observed to accompany ENSO (Chen 2002) and connected to northern India (Ding and Wang 2005; Yadav 2009a, b). The positive and negative pressure anomalies over the northwest of India and west tropical Indian Ocean, respectively, give rise to significant anomalous northeasterly winds over India subcontinent that are relatively cool and dry. Their interaction results in the upper-troposphere northeasterly air sinking, forcing the comparatively lighter, moisture laden lower-level southerly/southeasterly monsoonal flow upward. Thus, strong convection ensues over north central India (Yadav and Roxy 2019).

Further, to assess the impact of upper-level GPH gradient on the north central ISM region, we isolated the 250-hPa GPH data from the significant correlations in Fig. 3b (boxed areas of 50° E–80° E, 25° N–45° N and 40° E–65° E, 5° S–10° N). Even though the GPH over the two regions are poorly correlated (r = 0.157, 1948–2016), their meridional gradient (north minus south, Fig. 3b) is strongly correlated to the northern ISM rainfall (r = 0.47, significant at 99.9% level). Time series of this GPH gradient is shown in Fig. 2b, indicating that this gradient setup and associated 250-hPa zonal and meridional winds steers a northeasterly

wind that affects north central India rainfall. This relationship would later serve as a dynamic linkage between the changing Atlantic and Pacific influences on the north central ISM rainfall.

Next, we investigated the long-term variation of the north central ISM rainfall by computing the 21-year sliding correlation with the Topical Pacific SST Dipole index, calculated by the difference between the northeast of Australia and the north-equatorial Pacific index (hereafter referred as TPD), as both these indexes are anti-correlated among themselves (Folland et al. 2002). The sliding correlation (Fig. 4a, blue line) shows weak positive correlation upto late-1940s. The relationship was significantly positive from late-1940s to late-1970s. Thereafter, it shows a gradual weakening of

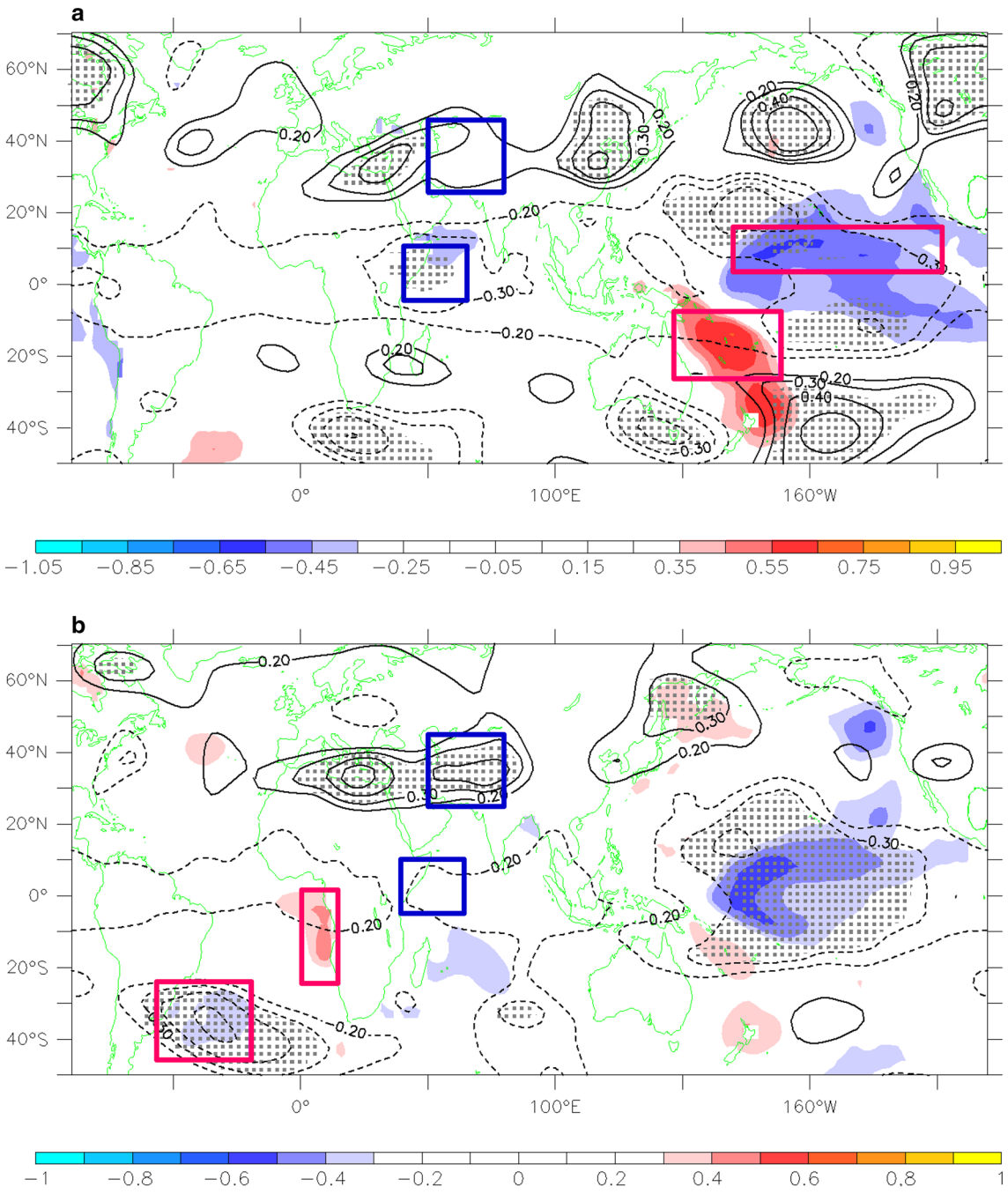

Fig. 5 Contiguous correlation of north central ISM with SST (color shaded) and 250-hPa GPH (contours) for the (**a**) period 1 and (**b**) period 2. The blue boxes depict the 250-hPa pressure gradient regions and pink boxes SST dipoles. The color shade and grey dots of contours are above 95% significant level

the relationship, especially from the late-1970s. Significant long-term changes in the distribution of tropical Pacific SST around the late-1970s, as was reported previously by Graham (1994), Trenberth and Hurrell (1994) could have some connection with the correlation change shown in Fig. 4a. Moreover, changes in teleconnections and circulation patterns around the late-1970s have also been observed (Ding et al. 2010; Lin et al. 2010; Qu and Huang 2012; Zhou et al. 2009; Yu and Zhou 2007). The mechanism by which this decadal variational shifts as occurred is examined in the ensuing analyses.

3.2 Change in the interannual variations

To examine the differences in circulation features associated with the decadal variation in the north central ISM rainfall's modulators, we constructed correlations and regressions for two time slices; i.e. 1948–78 (31 years of length –period 1) and 1979–2016 (38 years of length – period 2). Referencing Fig. 5, the observed differences in the north central ISM correlation patterns between periods 1 and 2 are: (a) the SST correlation in the Pacific for period 1 is distinctly stronger compared to period 2, (b) the 250-hPa low pressure anomaly is significant at west tropical Indian Ocean (period 1) while in period 2, the positive correlation at northwest of India is stronger, (c) in period 2, the south Atlantic shows a distinctive SST dipole pattern characterized by a positive correlation over the eastern tropical Atlantic and negative correlation over southwest Atlantic; this is referred to as the sub-tropical south Atlantic dipole (SAD) (Nnamchi et al. 2016) that is absent in period 1. Finally, the CGT pattern is visible in both periods but is more extensive in period 1 compared to period 2.

What is more, the 21-year sliding correlation between the north central ISM and the SAD (Fig. 4a, red line) shows positive correlation upto 1930s, then weak negative correlation upto 1980s and then a steady strengthening of the positive relationship, especially from the late-1970s. After the late-1970s the SAD-north central ISM relationship reverts to one that is both positive and significant. Moreover, it is interesting to note that, while the TPD is no longer significant, the SAD attained significance and this indicates an increasing combined effect of TPD and SAD on the north central ISM. The 21-year sliding correlation between TPD and SAD (Fig. 4a, green line) also indicates significant positive correlation between 1880s and 1930s and weak relationship between 1930s and 1970s and then a strengthening correspondence with each other after late-1970s, a previously undocumented feature. The technique of partial correlation has been used to remove the SAD from the contemporaneous TPD on the correlation between north central ISM and TPD in a statistical sense and vice versa for TPD removal. The 21-year sliding partial correlation between north central ISM and TPD after removing the SAD (Fig. 4b, cyan line) show similarly strong correlation prior to late-1970s and gradually become insignificant afterwards. The 21-year sliding partial correlation between north central ISM and SAD after removing the TPD (Fig. 4b, orange line) also switched around late-1970s. In both cases the partial correlations after removing the contribution of their counterpart are in good agreement with those without (Fig. 4a). It is important to note in the post late-1970s where SAD and TPD are inter-correlated among themselves, the influence of SAD remained after late-1970s for north central ISM. We have also plotted 21-year sliding correlation window for each of the dipole indexes (Fig. 4c). The south Atlantic dipole goes hand-by-hand with opposite correlation throughout the data period. But the Pacific dipole the north-equatorial SST box doesn't always follows the SST of north-east of Australia box. In the recent decades the drop of correlation of TPD

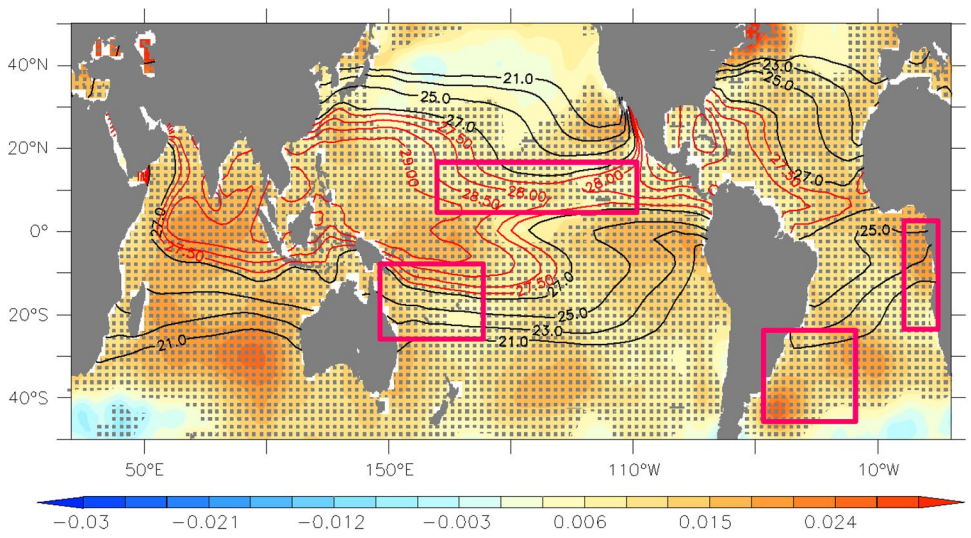

Fig. 6 SST trend analysis for the period 1948:2016 (shaded). Contours superimposed are the SST climatology (black contours for 21 – 27 °C with interval 2 °C, red contours for 27.5 °C above with interval 0.5 °C). The grey dots are SST trends significant at 95% confidence levels. The pink boxes represent the regions considered for tropical Pacific dipole (TPD) and south Atlantic dipole (SAD)

with rainfall is mainly from the SST of the north-east of Australia box.

To examine why the TPD seems to weaken its influence on north central ISM, we plotted the global SST trend for the entire period: 1948–2016 (Fig. 6). The SST shows significant increasing trend all along the tropics. The rising trend of SST over the equatorial and south-eastern tropical Atlantic has intensified the ITCZ over Atlantic and adjoining west Africa. The SAD is strongly related to the ITCZ of Atlantic and west Africa (Nnamchi et al. 2016; Yadav 2017b; Yadav et al. 2018) while the intensified ITCZ modulates the global circulation. Therefore, the influence of the SAD on the north central ISM, which has seemed to be overlooked before late-1970s, has become active afterwards. In the north equatorial Pacific, where the climatological SST is greater than 28°C and is strongly anti-correlated with north central ISM, a significant increasing SST trend prevails. Since the climatological SST is greater than 28°C, a slight increase or decrease in SST will affect a considerable bearing on available moisture and tropospheric heating and in doing so, the modulation of the large-scale circulation. Also, the increasing SST trend over the northern equatorial Pacific brings about an expansion of the Pacific warm-pool and so, convection intensification that is evident in the elevated tropical GPH height (Fig. 3b), which became unfavorable for north central ISM. In the southwest of the Atlantic, the climatological SST is below 20°C, therefore the increasing trend in SST in this region is less likely to have an impact on the atmospheric circulation.

To depict the TPD process, an analysis similar to Fig. 5 was conducted and is shown in Fig. 7. The difference in the correlation patterns between the TPD and SST indicates that significant SST warming was limited to the Pacific only (period 1). In period 2, significant SST warming has extended into areas in the Atlantic and Indian Oceans, i.e., into the equatorial western Pacific, the northwestern Pacific and northwest of Australia. What this advocates is that, in period 1, the La Niña was under the influence of a diminished warm-pool, while in period 2, the expanded warm-pool region likely initiated more intense and widespread. Furthermore, the sub-tropical south Atlantic dipole (Nnamchi et al. 2016; Yadav et al. 2018) is absent in period 1 but is revealed in period 2 (this is consistent with Fig. 4a, green line). The comparative spread of the warm-pool resulted in an increase in the tropospheric height, as was observed in Fig. 7b, evidenced by the lack of significance /reduced negative correlation of the 250-hPa GPH over the tropical Indian Ocean, Africa and Atlantic Ocean. This observation echoes the established La-Niña/El-Niño negative/positive GPH anomalies over the tropics due to tropical cooling/warming of SSTs (Yadav et al. 2010). In period 2, the Northern Hemisphere shows more patches of positive GPH correlations, representing a strong CGT pattern. This infers that the simultaneous occurrences of Atlantic Niño and La-Niña resulted in stronger CGT pattern in the Northern Hemisphere.

Next, correlation analysis for SAD was done for both periods (Fig. 8). For period 1, the 250-hPa GPH shows significant negative correlation over the mid-latitude Indian region and weak correlation over the tropical west Indian Ocean, which is unfavorable for the development of the northern ISM (this is consistent with Fig. 4a, red line). For period 2, the mid-latitude/extra-tropics region of the Northern Hemisphere shows areas of significant positive correlations corresponding to the CGT pattern. The La-Nina-type pattern is present. The Atlantic Dipole intensifies the Atlantic and west African ITCZ, which in turn produces a standing wave encircling north Africa, Mediterranean and Europe; this is observed as alternating negative and positive GPH anomalies over tropical Atlantic and Africa, the Mediterranean and northwestern Europe as the background jet stream weakens in this region. As was noted by Ding and Wang (2007), the northwest of Europe is the center of action for the generation and propagation of the Eurasian wave/CGT pattern. Similarly, the SAD fosters positive GPH anomalies over the Northern Hemisphere mid-latitude/extra-tropics and intensifies the CGT pattern. The significant negative correlation over tropical Atlantic and Africa along with the western Indian Ocean is due to poleward displacement of upper-troposphere GPH – a result of the ITCZ intensification over the Atlantic and Africa. The intense ITCZ generates strong upper-tropospheric divergence which displaces the zonally elongated Tibetan anticyclone that extends into northern Africa; this creates a negative pressure anomaly this is similar to what was observed. Last but not least, the significant negative correlation over the tropical Indo-Pacific and African regions is due to the simultaneous occurrence of the Atlantic Niño and La-Niña.

3.3 Modeling exploration

To investigate the observed role of TPD- and SAD-type SST anomalies as was previously discussed, a series of the SPEEDY simulations were conducted (see Sect. 2). Compared with the control simulation which has a climatological SST, the TPD simulation has the SST anomalies (Fig. 9a and 1975as forcing) over the Pacific region (120° E–90° W, 30° S–20° N), whereas the SAD simulation has the SST anomalies (Fig. 9c and 1999 as forcing) over the Atlantic region (60° W–20° E, 50° S–10° N). The regional SST forcing was fixed in JJAS. An extra simulation named TPD + SAD was further performed by including the SST forcing over both the Pacific and Atlantic regions (i.e. TPD and SAD forcing in combination, Fig. 9e). The TPD + SAD simulation was examined as the case that the simultaneous occurrences of TPD and SAD have been observed since the late-1970s

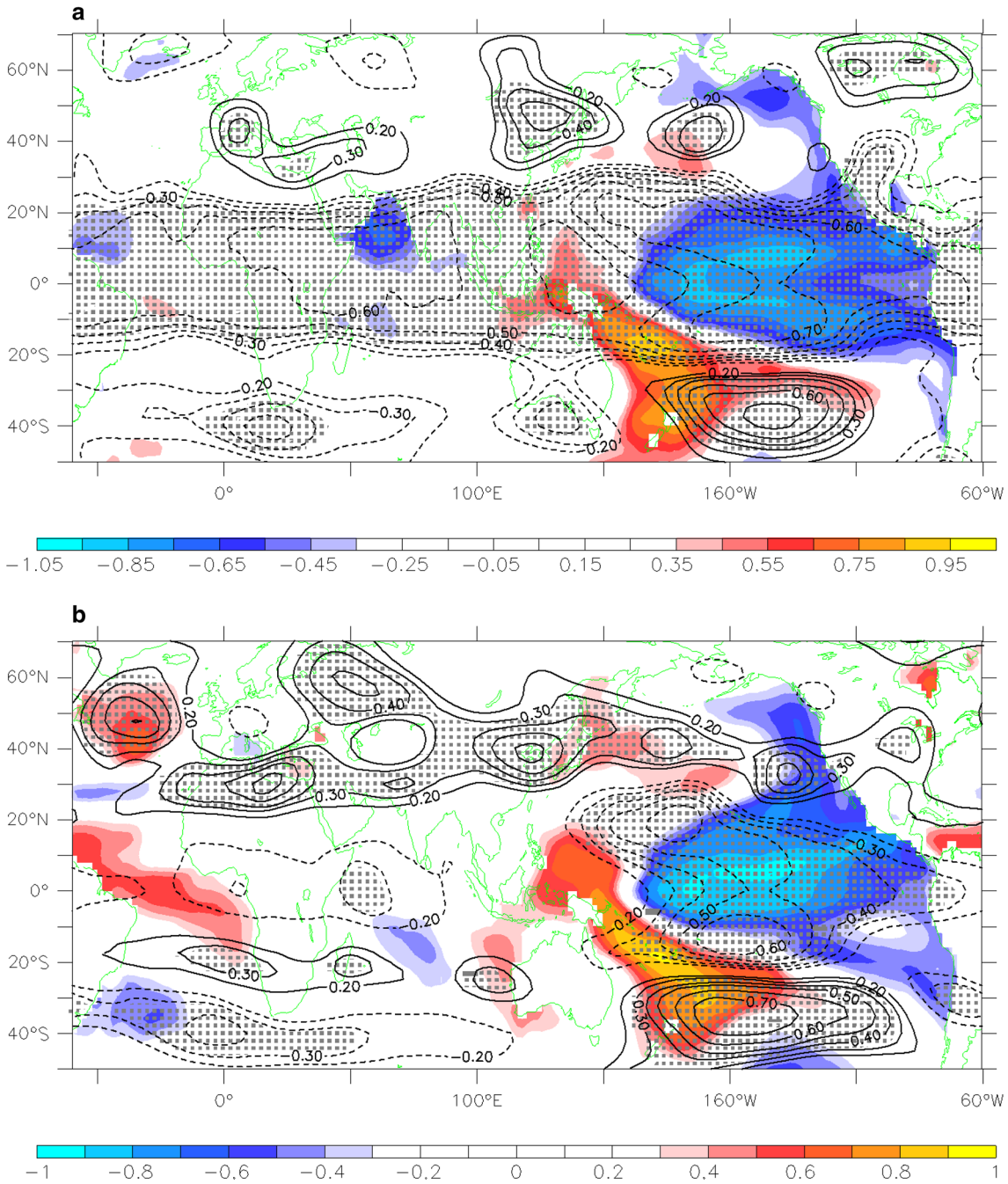

Fig. 7 Contiguous correlation of tropical Pacific dipole (TPD) with SST (color shade) and 250-hPa GPH (contours) for the (**a**) period 1 and (**b**) period 2. The color shade and grey dots of contours are above 95% significant level

(Rodriguez-Fonseca et al. 2009; Ding et al. 2012). The atmospheric responses to the SST anomalies can be explored when comparing the experimental simulations to the control simulation (Fig. 9b, d, and f). The model response was compared with the composite analysis for the excess minus deficient years the TPD and SAD composites (Fig. 9g–h).

The model response of TPD shows upper-troposphere (200-hPa) negative GPH anomaly along the tropics and positive anomaly over east Asia, which agrees with the composite analysis of TPD. The negative anomaly over tropics is over estimated, while the east Asia positive anomaly is under estimated. This lends support to the documented association of east Asia monsoon with La-Niña events via ISM (Ding and Wang 2005; Yadav 2009a, b). The northeasterly winds over the Indian subcontinent correspond to the upper-level divergence over tropical

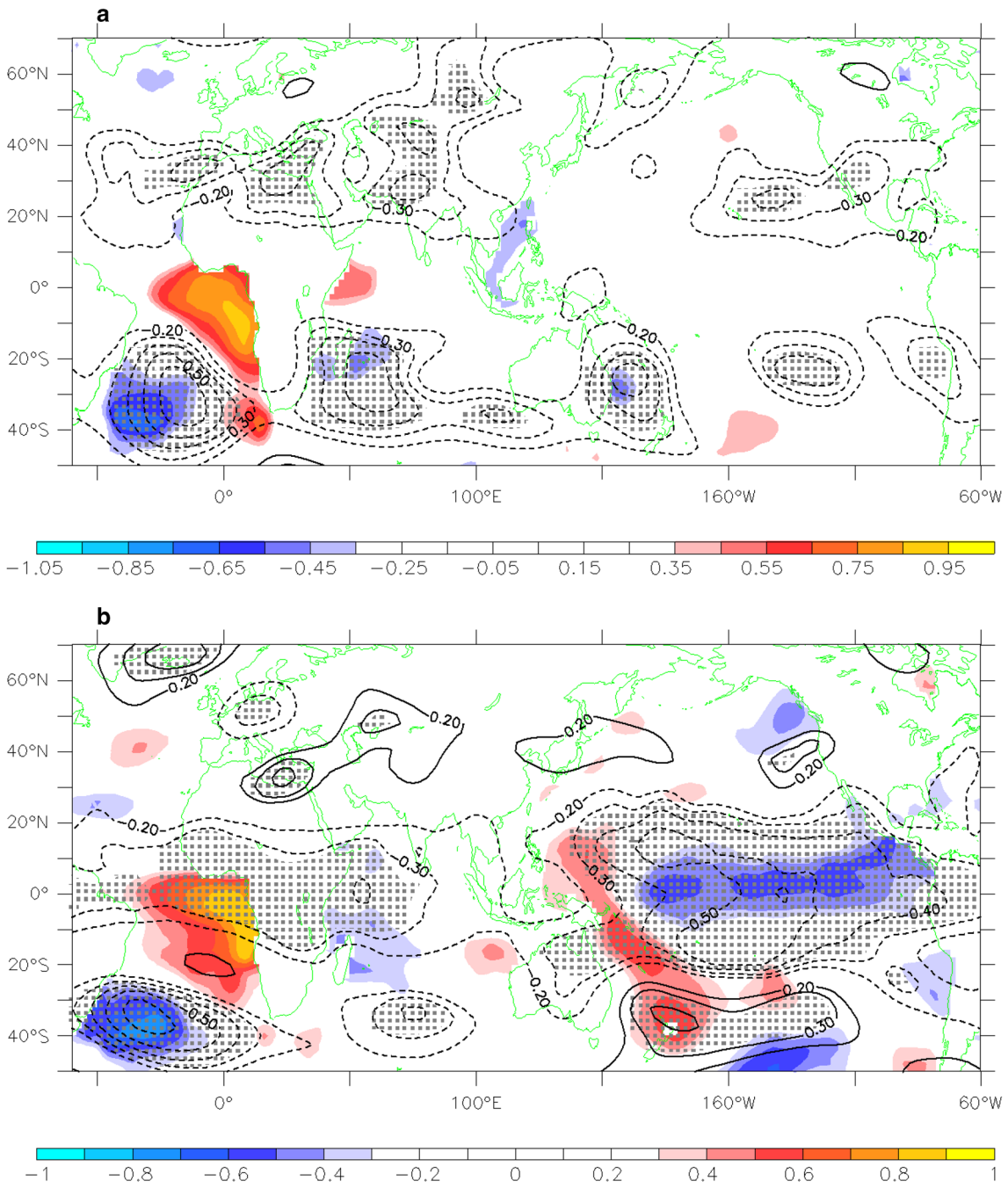

Fig. 8 Contiguous correlation of south Atlantic dipole (SAD) with SST (color shade) and 250-hPa GPH (contours) for the (**a**) period 1 and (**b**) period 2. The color shade and grey dots of contours are above 95% significant level

west Pacific, and negative GPH anomaly over tropical Indian Ocean. The decrease in SST over central equatorial Pacific and increase in SST over northeast of Australia reveals the contraction of warm-pool region resulting in strong convection and upper-troposphere divergence over warm-pool region. The SAD response (Fig. 9d) captures the Eurasian wave train similar to observation (Fig. 9h) consisting consecutive positive-negative GPH anomalies all along the upper-troposphere mid-latitude/extra-tropics but with reduced GPH anomalies. The positive anomaly along the tropical Atlantic and Africa represents strong convection elevating tropopause height (Fig. 9d). Caveats of the simulations do exits, since the model is not able to capture the poleward displacement of the zonally elongated Tibetan High over north Africa and Mediterranean,

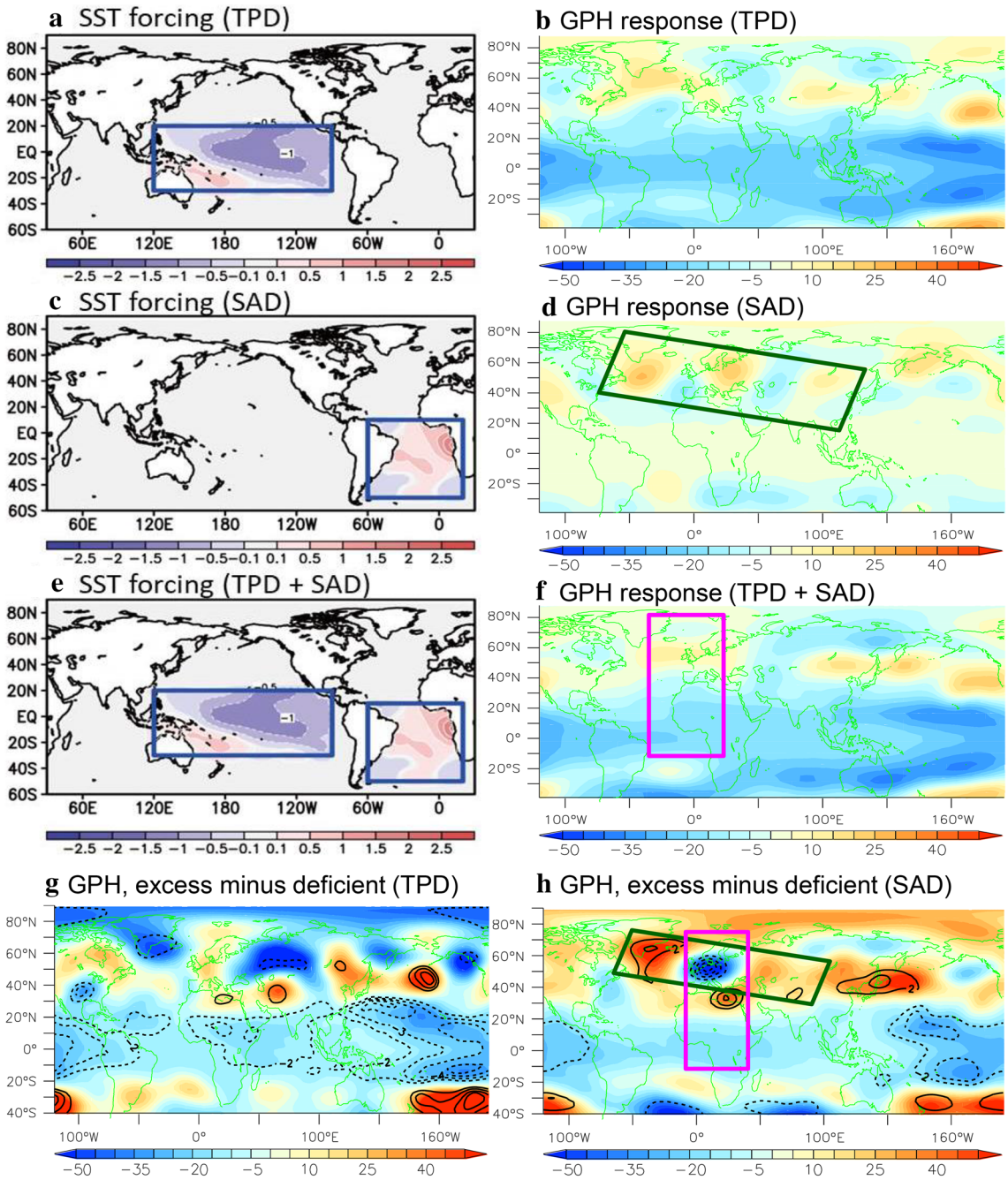

Fig. 9 SST anomalies for (**a**) TPD, (**c**) SAD and (**e**) TPD + SAD and 200-hPa GPH Model response to (**b**) TPD, (**d**) SAD and (**f**) TPD + SAD. The composite of 250-hPa GPH for excess–deficient (color shade) and significant (black contours) for (**g**) TPD during period 1 and (**h**) SAD for period 2. The green boxes in (**d**) and (**h**) represents the wave patterns and pink boxes in (**f**) and (**h**) represents the stationary waves

and meridional standing wave due to the upper troposphere strong divergence caused by the strong convection.

It has been observed that, after late-1970s, Atlantic Niño and La-Niña tended to occur simultaneously (Rodriguez-Fonseca et al. 2009; Ding et al. 2012). Therefore, to see the combined effect of both Atlantic Niño and La-Niña on the circulation pattern, we examined the compound simulation of both TPD and SAD. The compound response of TPD and SAD (Fig. 9f) appears to represent the meridional standing wave, with a slight poleward displacement in the GPH anomalies. The negative GPH anomaly over tropical Atlantic is the response of Pacific La-Nina effect lowering the tropical tropopause height, as observed in Figs. 9b and 7a. The Northern Hemisphere CGT pattern is also well captured in

the compound response. Overall, the model is able to capture the observed patterns with a slight shift.

3.4 Change in the synoptic processes

Synoptic disturbances are an important rain producer in this region. During this season (JJAS), numbers of tropical lows, depressions, deep depressions, storms and severe storms are formed in the north Indian Ocean. These systems generally move west-northwest direction towards the Indian landmass (Goswami 1987), produces heavy rainfall while imposing on the inter-annual variability of north central ISM. So, we have plotted the tracks of these storms obtained from "Tropical cyclone best track data site" maintained by Joint Typhoon Warming Centre (JTWC), USA along with the composite of SST and rainfall anomaly over India to get more insight into their relationship. Figure 10 shows the tracks of these systems, SST composite and composite rainfall anomaly for period 1 (Fig. 10a), period 2 (Fig. 10b), for the excess and deficient years of north central ISM (Fig. 10c, d), TPD (Fig. 10e, f) and SAD (Fig. 10g, h). In period 1, the storms were formed in the head Bay-of-Bengal (BoB) and moved westward/northwestward to north-west India. Comparatively, fewer storms were formed over north Arabian Sea. While, in period 2 the numbers of storms formed are comparatively much lesser than period 1, the storms were more scattered and quite good numbers shows more north ward movement. The average SST in the BoB and north and south of Arabian Sea is much warmer in period 2 than in period 1. The formation of storms not only depends upon the warmer SST but also upon the weaker wind shear, lower level convergence, strong convection and moisture supply. The warmer BoB in the post-79 was favorable for more production of storms, but the other parameters such as strong tropospheric wind shear were not suitable for the formation of the storms. Also, warmer SST shifted the ITCZ further south. The vortices formed along the ITCZ and further developed into storms were, therefore, observed mostly along the off-east coast of India and Arabian Sea.

During the excess north central ISM, TPD and SAD years, the storm paths were more zonal and the SST was relatively cooler than the deficient north central ISM, TPD and SAD years. In the deficient years, the storm tracks were more meridional and away from north India compared to excess years. In summary, during the excess years the storms are well organized, formed overhead Bay-of-Bengal (BoB) and migrates west-northwest direction towards south of north central India and the SSTs are cooler than the deficient years. While, during deficient years the storm are scattered, formed all along the eastern coast of India and quite good numbers of storm move northwards towards Bangladesh. The rainfall over north central India doesn't depends upon the numbers of storms formed during the season, but the position of storms formation and their direction of movements. The excess years represents the La-Niña type patterns when the warm-pool is more contracted and accompanied by the reduction of the Indian Ocean warming. On the other hand, the deficient years represents the El-Niño type patterns when the warm-pool is zonally elongated and the tropical Indian Ocean is warmed. These changes shift the ITCZ to lower latitudes in the India Ocean scattering the storms all along the north Indian Ocean. Furthermore, during excess years (Fig. 10, left panels) the upper-troposphere anomalous winds are northeasterlies, reducing the tropospheric wind shear over north India while allowing more frequent intrusion of comparatively cold and dry air masses from mid-latitude. This produces favorable conditions for the storms to form in the BoB and moves west-northwest direction. While, during deficient years (Fig. 10, right panels), the anomalous westerlies increase the tropospheric wind shear and hinders the intrusion of mid-latitude air masses. This also steers the westward moving storms to turn eastward under the influence of westerly, taking the storms away from north India (Wang et al. 2013). This confirms our hypothesis how anomalous northeasterly over Indian sub-continent are important for the storms track dynamics and for the convective activities over north India.

4 Conclusion and discussion

The current study attempts to explain the apparent change in the teleconnections of north central India summer monsoon rainfall before and after the late-1970s. The analysis shows that the north central ISM rainfall undergoes the combined effect of the interaction between the lower-level monsoonal flow and the upper-tropospheric meridional wind and it is significantly correlated to remote forcing of the Pacific and Atlantic SST dipoles. The La Niña-type pattern in the Pacific acts to reduce the tropopause height across the tropics, creating upper-troposphere negative GPH anomaly at the tropical west Indian Ocean. This circulation setup accompanies anomalous northeasterly over India, favorable for the north central ISM rainfall. The Atlantic dipole intensifiers the Atlantic and west Africa ITCZ, which generates stationary wave at the upper-troposphere while affecting the GPH anomaly of northwest Europe. A Eurasian wave train is then generated across central Asia, revealing a structure that resembles the CGT pattern. The CGT then creates positive GPH anomalies over mid-latitude/extra-tropics, favorable for north central ISM rainfall.

Earlier studies (Ramaswamy 1956, 1962; Ramamurthy 1969; Krishnamurti et al. 1980; Raman and Rao 1981) have reported that the summer monsoon is active over north India when the monsoon trough shifts northwards towards the foot hills of Himalayas. Occasionally, high amplitude

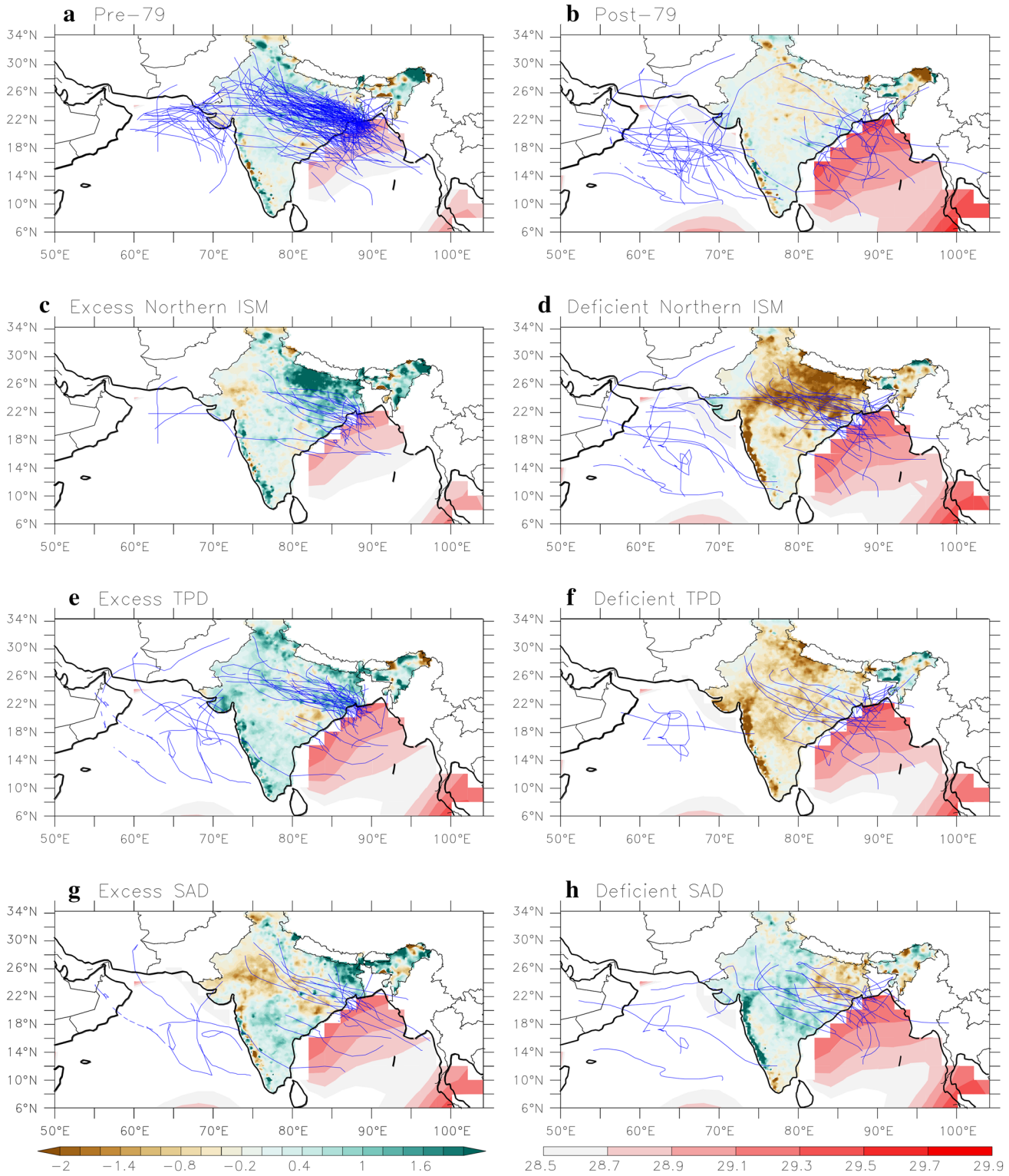

Fig. 10 Storm track plot (blue curves), SST composites (red shade) and rainfall composite anomaly (green-brown shade) for the **a** period 1: 1948–1978, **b** period 2: 1979–2006, **c** excess and **d** deficient north central ISM years, (**e**) excess and (**f**) deficient tropical Pacific dipole (TPD) years, and (**g**) excess and (**h**) deficient south Atlantic dipole (SAD) years

upper-tropospheric westerly trough intrudes into the northern parts of India, reinforcing the outbreak of convective activities. The current study adds further details to those findings by showing that the upper-troposphere anomalous positive and negative GPH over northwest of India and tropical west Indian Ocean, respectively, are associated with northeasterly over Indian sub-continent that is favorable for north central ISM. These regional upper-troposphere pressure anomalies have remained unchanged over the entire analysis period, but their connection with remote oceanic forcing have changed from one that was mostly affected by La-Niña to another that is collectively modulated by the subtropical south Atlantic dipole patterns.

Acknowledgements The data have been taken from(https://www.esrl.noaa.gov/psd/data/gridded/data.ncep.reanalysis.html, https://www.esrl.noaa.gov/psd/data/gridded/data.noaa.ersst.v3.html and ftp://www.tropmet.res.in/pub/data/rain/iitm-subdivrf.txt) and all data sources are duly acknowledged. Computational and graphical analyses required for this study have been completed with the free software xmgrace, NCL and Ferret.

Funding This research was funded by Indian Institute of Tropical Meteorology, Pune, India, Grant no [0098].

References

Ambrizzi T, Hoskins BJ, Hsu H-H (1995) Rossby wave propagation and teleconnection patterns in the austral winter. J Atmos Sci 52:3661–3672

Annamalai H, Liu P (2005) Response of the Asian summer monsoon to changes in El Niño properties. Quart J R Meteor Soc 131:805–831. https://doi.org/10.1256/qj.04.08

Chen T-C (2002) A North Pacific short-wave train during the extreme phases of ENSO. J Clim 15:2359–2376

Ding Q-H, Wang B (2005) Circumglobal teleconnection in the Northern Hemisphere summer. J Clim 18:3483–3505

Ding Q-H, Wang B (2007) Intraseasonal teleconnection between the summer Eurasian wave train and the Indian monsoon. J Clim 20:3751–3767

Ding Q-H, Wang B (2009) Predicting extreme phases of the India summer monsoon. J Clim 22:346–363

Ding R, Ha KJ, Li JP (2010) Interdecadal shift in the relationship between the East Asian summer monsoon and the tropical Indian Ocean. Clim Dyn 34(7–8):1059–1071

Ding H, Keenlyside NS, Latif M (2012) Impact of the equatorial Atlantic on the El Niño–Southern oscillation. Clim Dyn 38:1965–1972. https://doi.org/10.1007/s00382-011-1097-y

Folland CK, Renwick JA, Salinger MJ, Mullan AB (2002) Relative influences of the Interdecadal Pacific Oscillation and ENSO in the South Pacific Convergence Zone. Geophys Res Lett 29(13):1643. https://doi.org/10.1029/2001GL014201

Gershunov A, Schneider N, Barnett T (2001) Low-frequency modulation of the ENSO–Indian monsoon rainfall relationship: signal or noise? J Clim 14:2486–2492. https://doi.org/10.1175/1520-0442

Goswami BN (1987) A mechanism for the west-north-west movement of monsoon depressions. Nature 326(26):376–378

Graham NE (1994) Decadal-scale climate variability in the tropical and North Pacific during the 1970s and 1980s: observations and model results. Clim Dyn 10:135–162

Hoskins BJ, Ambrizzi T (1993) Rossby wave propagation on arealistic longitudinally varying flow. J Atmos Sci 50:1661–1671

Huang B, Peter W, Thorne etal (2017) Extended reconstructed sea surface temperature version 5 (ERSSTv5), upgrades, validations, and intercomparisons. J Clim 30:8179-8205,. https://doi.org/10.1175/JCLI-D-16-0836.1

Jin Q, Wang C, (2017) A revival of indian summer monsoon rainfall since 2002. Nat Clim Change 7(8):587–595 https://doi.org/10.1038/NCLIMATE3348

Kalnay E, Kanamitsu M, Kistler R, Collins W, Deaven D, GandinL,Iredel M, Saha S, White G, Woollen J, Zhu Y, ChelliahM,Ebisuzaki W, Higgins W, Janowiak J, Mo KC, RopelewskiC,Wang J, Leetmaa A, Reynolds R, Jenne R, Joseph D (1996) The NCEP/NCAR 40-year reanalysis project. Bull Am Meteor Soc 77:437–471

Kinter JL, Miyakoda K, Yang S (2002) Recent change in the connection from the Asian monsoon to ENSO. J Clim 15:1203–1215. https://doi.org/10.1175/1520-0442

Krishna Kumar K, Rajagopalan B, Cane MA (1999) On the weakening of relationship between the Indian monsoon and ENSO. Science 284:2156–2159. https://doi.org/10.1126/science.284.5423.2156

Krishna Kumar K, Rajagopalan B, Hoerting M, Bates G, Cane M (2006) Unraveling the mystery of Indian monsoon failure during El-Nino. Science 314:115–119

Krishnamurthy V, Goswami BN (2000) Indian monsoon–ENSO relationship on interdecadal timescale. J Clim 13:579–595. https://doi.org/10.1175/1520-0442

Krishnamurti TN, Ardanuy P (1980) The 10–20 day westward propagating mode and breaks in monsoon. Tellus 32:15–26

Kucharski F, Molteni F, Bracco A (2006) Decadal interactions between the western tropical Pacific and the North Atlantic Oscillation. Clim Dyn 26:79–91

Kucharski F, Bracco A, Yoo J, Molteni F (2008) Atlantic forced component of the Indian monsoon interannual variability. Geophys Res Lett 35:L04706. https://doi.org/10.1029/2007GL033037

Lin ZD, Lu RY, Zhou W (2010) Change in early-summer meridional teleconnection over the western North Pacific and East Asia around the late 1970s. Int J Climatol 30(14):2195–2204

Molteni F (2003) Atmospheric simulations using a GCM with simplified physical parametrizations. I. Model climatology and variability in multi-decadal experiments. Clim Dyn 20:175–191

Nnamchi HC, Li JP, Kucharski F, Kang I-S, Keenlyside NS, Chang P, Farneti R (2016) An equatorial–extratropical dipole structure of the Atlantic Ni˜no. J Clim 29:7295–7311

Pai DS, Sridhar L, Badwaik MR, Rajeevan M (2014) Analysis of the daily rainfall events over India using a new long period (1901–2010) high resolution (0.25° × 0.25°) gridded rainfall data set. Clim Dyn.https://doi.org/10.1007/s00382-014-2307-1

Parthasarathy B, Munot AA, Kothawale DR (1995) All India monthly and seasonal rainfall series: 1871–1993. Theor Appl Climatol 49:217–224

Qu X, Huang G (2012) An enhanced influence of tropical Indian ocean on the South Asia High after the Late 1970s. J Clim 25(20):6930–6941

Ramamurthy K (1969) Monsoons of India, some aspects of the 'Break in the Indian southwest monsoon during July and August. Forecasting Manual No. IV-18.3. India Meteorological Department, Pune.

Raman CRV, Rao YP (1981) Blocking highs over Asia and monsoon droughts over India. Nature 289:271–273

Ramaswamy C (1956) On the sub-tropical jet stream and its role in the development of large scale convection. Tellus 8:26–60

Ramaswamy C (1962) Breaks in the Indian summer monsoon as a phenomenon of interaction between the easterly and the subtropical westerly jet streams. Tellus 14:337–349

Rodríguez-Fonseca B, Polo I, García-Serrano J, Losada T, Mohino E, Mechoso CR, Kucharski F (2009) Are Atlantic Niños enhancing Pacific ENSO events in recent decades? Geophys Res Lett 36:L20705. https://doi.org/10.1029/2009GL040048

Torrence C, Webster PJ (1999) Interdecadal changes in the ENSO–monsoon system. J Clim 12:2679–2690. https://doi.org/10.1175/1520-0442

Trenberth KE, Hurrell JW (1994) Decadal atmosphere ocean variations in the Pacific. Clim Dyn 9:303–319

Vellore RK, Krishnan R, Pendharkar J, Choudhary AD, Sabin TP (2014) On the anomalous precipitation enhancement over the Himalayan foothills during monsoon breaks. Clim Dyn 43:2009–2031. https://doi.org/10.1007/s00382-013-2024-1

Wang S-Y, Davies RE, Huang W-R, Gillies RR (2011) Pakistan's two-stage monsoon and links with the recent climate change. J Geophys Res 116:D16114

Wang S-Y, Buckley B, Yoon J-H, Fosuâ B (2013) Intensification of pre-monsoon tropical cyclones in the Bay of Bengal and its impacts on Myanmar. J Geophys Res 118:1–12. https://doi.org/10.1002/jgrd.50396

Wu CH, Wang SY, Hsu HH (2018) Large-scale control of the Arabian Sea monsoon inversion in August. Clim Dyn 51(7):2581–2592. https://doi.org/10.1007/s00382-017-4029-7

Yadav RK (2009a) Changes in the large-scale features associated with the Indian summer monsoon in the recent decades. Int J Climatol 29:117–133. https://doi.org/10.1002/joc.1698

Yadav RK (2009b) Role of equatorial central Pacific and northwest of North Atlantic 2-metre surface temperatures in modulating Indian summer monsoon variability. Clim Dyn 32:549–563. https://doi.org/10.1007/s00382-008-0410-x

Yadav RK, Yoo JH, Kusharski F, Abid MA (2010) Why is ENSO influencing northwest India winter precipitation in recent decades? J Clim 23:1979–1993. https://doi.org/10.1175/2009JCI3202.1

Yadav RK (2017) On the relationship between east equatorial Atlantic SST and ISM through Eurasian wave. Clim Dyn 48:281–295. https://doi.org/10.1007/s00382-016-3074-y

Yadav RK, Srinivas G, Chowdary JS (2018) Atlantic Niño modulation of the Indian summer monsoon through Asian jet.npj. Clim Atmos Sci 1:23. https://doi.org/10.1038/s41612-018-0029-5

Yadav RK, Roxy MK (2019) On the relationship between north India summer monsoon rainfall and east equatorial Indian Ocean warming. Glob Planet Change 179:23–32. https://doi.org/10.1016/j.gloplacha.2019.05.001

Yu R, Zhou T (2007) Seasonality and three-dimensional structure of interdecadal change in the East Asian Monsoon. J Clim 20(21):5344–5355

Zhou T et al (2009) Why the Western Pacific subtropical high has extended westward since the late 1970s. J Clim 22(8):2199–2215